Grafting well-defined polymers onto unsaturated PVDF using thiol-ene reactions

Ting-Chih Lin [a], Piotr Mocny [a], Martin Cvek [a,b], Mingkang Sun [a], Krzysztof Matyjaszewski [a,*]

[a] *Department of Chemistry, Carnegie Mellon University, 4400 Fifth Avenue, Pittsburgh, PA, 15213, USA*
[b] *Centre of Polymer Systems, Tomas Bata University in Zlín, Trida T. Bati 5678, 760 01, Zlin, Czech Republic*

ARTICLE INFO

ABSTRACT

Poly(vinylidene fluoride) (PVDF) is commonly used in membranes, lithium-ion battery binders, and coatings due to its thermal and chemical robustness. Nevertheless, PVDF-based copolymers can broaden the application scope and performance capabilities of pristine PVDF. PVDF has been modified via grafting-from reactions. However, grafting density and graft length, two important properties of graft copolymers, cannot be accurately determined. Herein, we used *grafting-onto* thiol-ene reactions as a method to modify PVDF. The molar mass of pre-synthesized, thiol-terminated polymers were accurately determined, and grafting densities were calculated. Unsaturated sites were generated through dehydrofluorination and dehydrochlorination in PVDF and P(VDF-*co*-chlorotrifluoro-ethylene) (PVDF-CTFE). Various conditions were studied, including the molar mass and chemical structure of grafts, the degree of thiol substitution, and thiol-ene reaction mechanisms. Base-catalyzed Michael addition with secondary thiols performed best, with the highest grafting density calculated to be about 4 chains per PVDF chain. Despite the low grafting density, changes in material properties between the product and starting materials were observed, validating this controlled method for PVDF modification.

1. Introduction

Fluoropolymers are robust polymers used in various applications. The strong electron-withdrawing property of the fluorine atoms on the backbone provides chemically and thermally resistant materials [1]. Poly(vinylidene fluoride) (PVDF) is a commercially available fluoropolymer, second in market value only behind polytetrafluoroethylene (PTFE) [2]. PVDF is commonly used in coatings [3], water filtration membranes [4–6], and in lithium-ion batteries as a filler and cathode binder [7–9]. In addition, PVDF displays very interesting electronic properties in the form of piezoelectricity, ferroelectricity, and triboelectricity [10] However, PVDF on its own is hydrophobic, and its crystalline nature makes it difficult to process. By functionalizing PVDF via macromolecular engineering, one can tune its polarity, and mechanical and electronic properties. There have been many reports of attempts to modify PVDF as a block or graft copolymer [5,9,11–13]. In general, graft copolymers tend to retain more properties of their parent polymers than statistical copolymers, which would be more optimal for retaining the chemical robustness and electronic properties of PVDF. Graft copolymers have been synthesized via three different routes: (i) grafting from a backbone containing initiation sites; (ii) grafting

well-defined chain-end functionalized polymers onto reactive sites in the backbone; or (iii) grafting through macromonomers [14,15]. PVDF was reported to be functionalized via grafting from reactions, using the C–F bond as an alkyl halide initiator for atom transfer radical polymerization (ATRP) [9,11,16]. However, the bond dissociation energy of a C–F bond is well over 400 kJ/mol. Compared to a C–Cl bond, which has a bond dissociation energy of around 300 kJ/mol, the cleavage of the C–F bond by the copper complex needed to generate a radical is difficult [17]. Additionally, the copper-fluoride complex formed in this activation has a very low rate constant of deactivation [18]. The factors stated above make it challenging to accurately determine the grafting density and graft length, two parameters that determine the properties of grafted materials.

Dehydrofluorination of PVDF introduces unsaturation [19–21], which may be targeted by radical addition as well as thiol-ene reactions. In the most common strategy, *solid* dehydrofluorinated PVDF (e.g., a membrane) was exposed to a mixture of (meth)acrylic monomers and a radical initiator [22–28]. In this process, propagating macroradicals are grafted through unsaturations of PVDF. In thiol-ene strategy, thiols and radical initiators were used, and the generated thiol radical reacted via addition reaction [29–36]. While both strategies are similar, the

thiol-ene reaction is less effective because the unsaturation sites of PVDF are deactivated by strong electron withdrawing fluorine groups [33]. In fact, a specially designed variant of PVDF bearing CH=CH (dehydrofluorinated P(VDF-co-TrFE)) proved to be much more active than typical PVDF with CH=CF groups. Unless this variant was used, a much better solution was to use thiol-ene reaction under basic conditions [32], i.e., Michael addition, which is known to react with electron-deficient alkenes [37,38]. This chemistry was rarely used in the context of graft copolymers, despite the rich literature on crosslinking of PVDF with similar chemistries [39]. Radical curing was typically used on iodinated or brominated PVDF (e.g., a copolymer of VDF with bromotrifluoroethylene) that is susceptible to peroxide radicals [2,40]. Usually, crosslinking of PVDF-based polymers was carried out via nucleophilic reactions, i.e., with diamines (predominant until the late 1960s) and bisphenols (current method) [39]. The addition of thiol species onto PVDF remains relatively unexplored, and to the best of our knowledge, there are no grafting-onto examples that use thiol chain-end functionalized polymers.

Therefore, this chemistry was employed to prepare loosely grafted PVDF comb polymers using unsaturated PVDF-based materials and thiol chain-end functionalized polymers. One obstacle was that double bond formation on dehydrofluorinated PVDF is poorly defined, since it is an auto-catalyzed reaction [41]. This may lead to the formation of conjugated structures, which would explain the color change (red, brown, and black) observed in the material [24]. Head-head/tail-tail defects present in PVDF were previously recognized as more reactive sites for grafting. This effect was rationalized by increased steric strain imposed by F atoms [42]. However, as F is only 8% larger than H atom, other, such as electronic, effects may also play an important role. As such, these defect sites are likely more vulnerable to dehydrofluorination. Dehydrochlorinated PVDF-CTFE was also selected as a backbone material. Dehydrochlorination of PVDF-CTFE with amines was reported to be a much milder method to modify PVDF-based materials while avoiding the main chain scission that may occur when dehydrofluorinating PVDF with stronger bases [29]. It is important to note that there is a range of reactivity ratios between CTFE and VDF in the literature, including those close to unity, $r_{VDF} = 0.73$ and $r_{CTFE} = 0.75$ [43], but also those indicating lower reactivity of VDF than CTFE, $r_{VDF} = 0.17$ or 0.069 and $r_{CTFE} = 0.52$ or 0.80, respectively [44,45]. Apparently, industrially, CTFE could be added as a continuous or semi-continuous feed to the VDF-containing reactor to provide a more statistical distribution of CTFE units in copolymer chains. This, however, could also be accompanied by the presence of PVDF rich fraction at high monomer conversion, which can impact some material properties discussed later in the text.

Thiol-ene click reactions can occur through two different mechanisms – radical addition and nucleophilic Michael addition [46]. Radical addition requires the use of a radical source, either thermal- or photoinitiated, and an oxygen-free environment. Michael additions can occur under basic conditions with mild heating and was more effective for fluorinated materials [32]. However, bases in the reaction can further promote dehydrohalogenation. Besides the addition mechanism, one must also consider the impact of steric effects on grafting efficiency. There are several factors that can play a role in thiol-ene grafting-onto reactions. First, the steric bulkiness of the large macromolecule can affect the accessibility and contact between the thiol and alkene. Second, the substitution of the thiol, which has both a steric and electronic effect on the thiolate anion/radical, can also affect grafting efficiency. The effects of these parameters on grafting-onto performance have not been previously explored. We addressed this by investigating reactions of well-defined primary, secondary, and tertiary thiol chain-end terminated poly(meth)acrylate polymers with dehydrofluorinated and dehydrochlorinated PVDF-based polymers. We evaluated the reaction performance and its kinetics and characterized the obtained materials to study the effect of grafts on physicochemical properties.

2. Experimental

2.1. Materials

Poly(vinylidene fluoride-*co*-chlorotrifluoroethylene) (P(VDF-CTFE) copolymer CTFE, (percentage of CTFE units of 10 wt%, i.e., 5.8 mol%, M_n of 92,400; PolyK), 4-cyano-4-[(dodecylsulfanylthiocarbonyl)sulfanyl]pentanoic acid (CDSPA, 97%, Boron Molecular), tributylphosphine (97%), hydrazine (anhydrous, 98%, Sigma-Aldrich), triethylamine (TEA, 99%, Sigma-Aldrich), 2-hydroxyethyl disulfide (technical grade, Sigma-Aldrich), α-bromoisobutyryl bromide (98%, Sigma-Aldrich), 2-hydroxy-4'-(2-hydroxyethoxy)-2-methylpropiophenone (Irgacure 2959, 98%, Sigma-Aldrich), toluene (99.8%, Sigma-Aldrich) were used as received. N, N-dimethylformamide (DMF, certified), methanol (MeOH, certified), tetrahydrofuran (THF, certified), methylene chloride (DCM, certified), hexanes (certified), and ethyl acetate (certified) were used as received from Fisher Chemical. Copper (II) bromide (CuBr$_2$, 99.99%), tris(2-pyridylmethyl)amine (TPMA, 97%, AmBeed), tris[2-(dimethylamino) ethyl]amine (Me$_6$TREN, 97%, Thermo Scientific), tin(II) 2-ethylhexanoate (Sn(EH)$_2$, technical grade, Thermo Scientific), anisole (99%, TCI), dimethyl sulfoxide-d_6 (DMSO-d_6, 99.96%, CIL), chloroform-d (CDCl$_3$, 99.96%, CIL), acetone-d_6 (99.96%, CIL) were used as received. Polystyrene standard ($M_n = 1,052,000$, $M_w = 1,119,000$, Đ = 1.06) was used as received from Scientific Polymer Products.

Methyl methacrylate (MMA, 99%, Sigma-Aldrich) and methyl acrylate (MA, 99%, Sigma-Aldrich) were passed through a basic alumina plug prior to use to remove inhibitor.

Azobisisobutyronitrile (AIBN, 98%, Sigma-Aldrich) was recrystallized in methanol prior to use.

Dehydrofluorinated PVDF (percentage of dehydrofluorinated VDF units of 6.4 wt%, i.e., 9 mol%, M_n of 121,000) was generously provided by Professor Henry Sodano from the University of Michigan.

2.2. Synthesis of bis 2-(α-bromoisobutyryloxy)ethyl disulfide (BIBOED)

The synthesis of bis 2-(α-bromoisobutyryloxy)ethyl disulfide (Scheme 1) was performed following the literature procedure [47]. 2-Hydroxyethyl disulfide (5g, 1 eq.), α-bromoisobutyryl bromide (10 mL, 2.5 eq.), triethylamine (11 mL, 2.5 eq.), and 45 mL DCM were added to a dry round bottom flask under an inert atmosphere. The reaction mixture was left to stir overnight at room temperature. The product was purified by filtration to remove salts formed during the reaction, then washed with HCl, sodium bicarbonate, water, and brine (100 mL × 2 each), dried with magnesium sulfate, and concentrated under vacuum. The concentrated crude product was then purified using flash chromatography.

2.3. Synthesis disulfide bridged poly(methyl methacrylate) (PMMA)

MMA was polymerized from BIBOED initiator using activators regenerated by electron transfer (ARGET) ATRP. Stock solutions of CuBr$_2$ (1.78 mg, 8 μmol, 0.04 eq.) and TPMA (9.28 mg, 32 μmol, 0.16 eq.) were prepared in DMF. Into a 25 mL Schlenk flask was added MMA (4 g, 40 mmol, 200 eq.), BIBOED (90 mg, 0.2 mmol, 1 eq.), CuBr$_2$ and TPMA stock solutions, and 60 vol% of anisole relative to the reaction mixture. The flask was sealed and purged with nitrogen for 20 min. A stock solution of Sn(EH)$_2$ (40 mg, 0.1 mmol, 0.5 eq.) in anisole was purged with nitrogen and added to the reaction mixture. The reaction was heated in a 60 °C oil bath to begin the reaction. After 3 h, the reaction was purged by opening the flask to the atmosphere. ^{1}H NMR showed roughly a 50% conversion. The mixture was then passed through a basic alumina plug to remove copper salts, precipitated into methanol, filtered under vacuum, and dried.

Scheme 1. Reaction scheme of bis 2-(α-bromoisobutyryloxy)ethyl disulfide (BIBOED).

2.4. Reduction of disulfide bridged PMMA

In a 25 mL round bottom flask, disulfide bridged PMMA (1 g, 0.1 mmol, 1 eq.) was dissolved in 10 mL of THF, and the reduction was initiated by the addition of tributylphosphine (207 mg, 1 mmol, 10 eq.) (Scheme 2). The reaction was monitored by GPC and stopped after 5 h. The reaction mixture was precipitated in methanol, filtered, and dried.

2.5. Synthesis of polymers via reversible addition-fragmentation chain-transfer (RAFT) polymerization

In general, monomer, AIBN, and CDSPA were added into a 25 mL Schlenk flask. The reaction mixture was then subjected to three freeze-pump-thaw cycles and finally filled with nitrogen. The reaction was then heated in a 60 °C oil bath to start the reaction. The reactions were stopped once a degree of polymerization of 80, determined by ^{1}H NMR of the crude reaction mixture, had been reached. The reaction was quenched by opening the flask to atmospheric oxygen, then precipitated in methanol, filtered, and dried under vacuum overnight.

2.6. Aminolysis of RAFT chain ends

In general, the polymer made by RAFT polymerization and 10 equivalents of hydrazine are added into a 25 mL round bottom flask, along with 2x the mass of DMF. The reaction proceeds for an hour at room temperature, upon which the solution will change from a yellow color to mostly transparent. The reaction is then precipitated in a 5% v/v methanol solution, redissolved, precipitated in methanol, filtered, and dried.

2.7. Synthesis of dehydrochlorinated (DHC) PVDF-CTFE

The synthesis of DHC-PVDF-CTFE was adapted from the literature procedure [29]. Into a 100 mL round bottom flask was added PVDF-CTFE (2 g, 1 eq.), TEA (174 mg, 1.7 mmol, 1 eq.), and 60 mL DMF. The reaction is heated at 50 °C for 24 h. The product is purified by precipitation in a 5% v/v HCl in methanol solution, redissolved, precipitated in regular methanol, then filtered and dried.

2.8. Grafting onto unsaturated PVDF materials – base catalyzed

In general, into a 25 mL round bottom flask is added PVDF material (1 g, 1 eq.), thiol-terminated polymer (0.5 g), TEA (1–2.2 eq.), and 10 mL DMF. The reaction mixture is heated in a 50 °C oil bath for 24 h. The aliquots were withdrawn at pre-determined time intervals. The product is purified by precipitation in a 5% v/v HCl in methanol solution, redissolved, precipitated in chloroform, then filtered and dried.

2.9. Grafting onto unsaturated PVDF materials – radical catalyzed

In general, in a 25 mL round bottom flask, PVDF material (1 g, 1 eq. of double bonds), thiol-terminated polymer (0.5 g), Irgacure 2959 (1 eq.), and 10 mL DMF are added. The reaction mixture is sparged with nitrogen for 15 min, then irradiated with a UV lamp (λ = 365 nm, 4.32 mW/cm^2). The product is purified by precipitation in methanol, redissolved, precipitated in chloroform, then filtered and dried.

2.10. Nuclear magnetic resonance

All ^{1}H and ^{19}F NMR spectra were acquired using a Bruker Avance III 500 MHz spectrometer with DMSO-d_6, CDCl$_3$, and acetone-d_6 used as the solvents.

2.11. Gel permeation chromatography (GPC)

Molar mass and molar mass distribution were determined using GPC. All samples were dissolved in the corresponding solvents, then filtered through alumina and a 0.45 μm PTFE filter. For samples containing TEA, the reaction was stopped by adding two drops of concentrated HCl before filtration. An Agilent GPC was equipped with a RI detector and PSS columns (Styrogel 10^5, 10^3, and 10^2 Å) with DMF as an eluent at 50 °C and a flow rate of 1 mL/min. The analogous GPC device using THF as an eluent at 35 °C and a flow rate of 1 mL/min was employed as well. Analysis of polymer signals was based on PSS WinGPC software (build 9666) for molar mass analysis. Both instruments used linear poly(methyl methacrylate) (PMMA) standards for calibration.

2.12. Monitoring grafting onto kinetics by GPC

Kinetic experiments were conducted using the same procedure as described in section 2.8, using DHC-PVDF-CTFE and PMA-SH (secondary thiol-terminated side chain). The reaction mixture was diluted twice to ensure homogeneity in the solution. Then, 15.6 mg of polystyrene standard was added. Aliquots were taken at specified time intervals and immediately quenched with HCl and passed through basic alumina before injecting into GPC. The GPC signals were deconvoluted by fitting with Gaussian distribution functions. Deconvolution is provided in the SI (Fig. S16).

2.13. Thermogravimetric analysis (TGA)

Thermogravimetric analysis (TGA) of the grafted PVDF products was conducted on a TGA550 (TA Instruments, Delaware, USA) under nitrogen atmosphere with a purge rate of 60 mL/min. The sample (10–15 mg) was placed onto a platinum pan (100 μL) and subjected to a defined thermal program. First, the temperature was increased to 120 °C at a rate of 30 °C/min, followed by the isothermal hold for 10 min to remove the volatile compounds. Afterwards, the temperature was increased at a rate of 10 °C/min until reaching 800 °C.

2.14. Differential scanning calorimetry (DSC)

DSC was conducted on the PerkinElmer DSC 4000 under nitrogen atmosphere with a flow rate of 20 mL/min. The sample (3–8 mg) was sealed in an aluminum pan and then subjected to two heating and cooling cycles. The temperature range scanned was −60 °C to 220 °C,
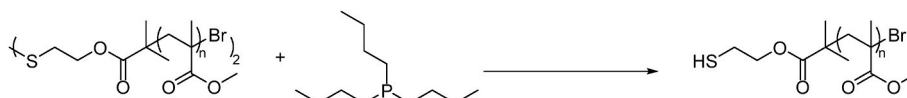
Scheme 2. Reduction of disulfide bridged PMMA using tributylphosphine.

with a rate of heat flow of 10 °C/min. An empty sample pan was used as a reference.

3. Results and discussion

Grafting-from macromolecules typically allows for the generation of grafts of high grafting density because of the low steric hindrance of reacting small monomer molecules. Controlled radical polymerizations produce grafts of desired chain lengths and narrow molar mass distributions. Generated polymers are exclusively grafted, and no free polymers should be removed, which simplifies purification procedures. However, grafting-from PVDF is not straightforward due to the slow initiation from its reactive sites. Moreover, the grafts cannot be easily cleaved, and the grafting density as well as the molar mass of the grafts are not accessible. To overcome these limitations, there have been efforts to use sacrificial initiators to control and monitor the polymerization from PVDF [48,49]. The initiators, however, are not a perfect match for the activity of the PVDF initiating sites. This can lead to faster growth from the sacrificial initiators, resulting in an inaccurate determination of side chain molar mass.

Since grafting from PVDF had many challenges and uncertainties, grafting onto PVDF was herein explored as an alternative method. Grafting-onto is rather straightforward, comparatively, as the grafts were analyzed prior to the grafting [50]. Additionally, purified grafted copolymers were analyzed by NMR to estimate the content of the grafted chains. DHF-PVDF was initially chosen as the starting material. Thiol-terminated polymers can react with the double bonds generated on the backbones using thiol-ene click reactions. The locations of unsaturation on DHF-PVDF are not well defined due to the auto-catalyzing nature of dehydrofluorination along the PVDF backbone [41]. DHC-PVDF-CTFE was also selected as a starting material for its milder dehydrochlorination conditions. This unsaturated material was synthesized using PVDF-CTFE with 10 wt% CTFE following a literature procedure [29].

3.1. Synthesis of thiol-terminated side chain polymers

Three different types of polymers were synthesized, each terminated by primary, secondary, and tertiary substituted thiols. PMMA was chosen for primary and tertiary thiols, and PMA for secondary thiols to keep structures as consistent as possible and easy to process (Scheme 3).

It is important to note that PMMA is miscible with PVDF and PVDF-based materials, which means the crystallinity may be disrupted, resulting in a loss of piezoelectricity [51,52]. All thiol-terminated polymers had a number average molar mass, M_n, of around 8,000–11,000 g/mol (Table 1). This range was selected to decrease the steric hindrance of sequentially grafted chains and to potentially analyze chain ends by NMR. Specific side chains and sample pairings are detailed in Table S1.

Tertiary and secondary thiol-terminated PMMA and PMA were prepared under similar conditions using reversible addition-fragmentation chain-transfer (RAFT) polymerization [53]. The trithiocarbonate chain end was transformed into a thiol via aminolysis. For the primary thiol-terminated polymers, a bifunctional, disulfide-linked ATRP initiator was synthesized following a previously reported procedure [47]. MMA was then polymerized from both initiation sites using ARGET

Table 1
Functionality, molar mass, and dispersity of synthesized thiol-terminated polymers.

Thiol substitution	M_n (g/mol)	M_w (g/mol)	Đ
Primary	11,800	16,200	1.37
	8,600	10,800	1.24
	7,500	9,750	1.30
Secondary	10,500	11,300	1.08
Tertiary	7,640	9,170	1.20
	8,890	11,030	1.15
	10,000	11,600	1.16

ATRP. The disulfide bond was reduced using tributylphosphine to yield primary thiols.

3.2. Grafting onto unsaturated PVDF using radical- and base-catalyzed thiol-ene reactions

One benefit of grafting-onto is that the pre-synthesized side chain polymers are very well defined, with known molar mass and dispersities. The molar mass and NMR spectra of the pre-synthesized polymers, PVDF, and final product were used to determine grafting efficiency and estimate the composition of copolymers. The general grafting-onto strategy is shown in Scheme 4.

The reactions were run with 1 g of PVDF starting material, 0.5 g of thiol-terminated polymer, and 0.1 equivalents of Irgacure 2959 under UV irradiation or 2.2 equivalents of triethylamine (TEA) at 50 °C. Equivalents of reagents were in relation to the amount of double bonds on the PVDF starting material. Initially, experiments were designed to use a 1:1 M ratio of alkenes to thiols. However, large masses of thiol-terminated polymers and a very small mass of PVDF were required for this balance. For experimental convenience, instead of 1:1 M ratio of alkene to thiol, we employed a ratio closer to 1:0.0356 or 0.148 for DHF-PVDF and DHC-PVDF-CTFE, respectively. This simplified the removal of unreacted polymers. At this scale, unreacted thiol-terminated linear polymers could be isolated from the reaction mixture. Table 2 lists all the reactions that were performed, as well as the calculated grafting efficiency.

The fraction of grafted polymers was calculated as follows: the P(M) MA peaks were integrated against the PVDF peaks (Fig. 1), then divided by the sum of the two integrations to get the molar fraction. The molar fraction was converted to a mass fraction using the molar mass of the linear polymers. Additional calculation details and remaining NMRs are provided in the supplementary information.

Based on the calculated values (Table 2), the base catalyzed mechanism had a grafting efficiency about an order of magnitude greater than the radical mechanism. In general, using DHF-PVDF as the backbone resulted in higher grafting efficiency due to conjugated structures having higher reactivity. This effect is especially prominent in samples S5–8. As we move to less reactive systems, such as more sterically hindered side chains (S5, 6) or radical-catalyzed thiol-ene reactions (S7, 8), we see enhanced grafting with DHF-PVDF.
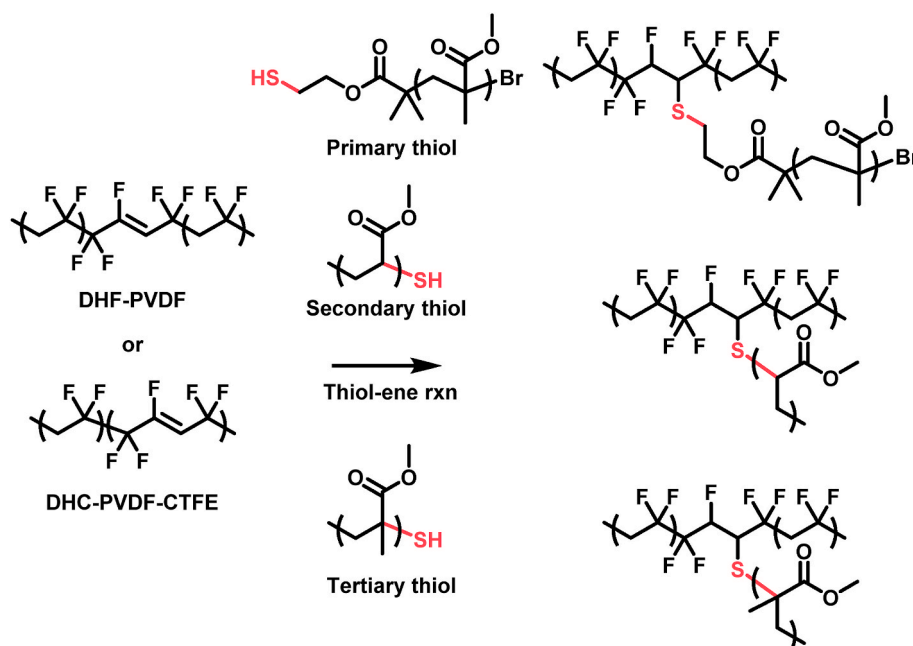
3.3. Thermogravimetric determination of grafting efficiency

Thermogravimetric analysis (TGA) was used, besides delineating the
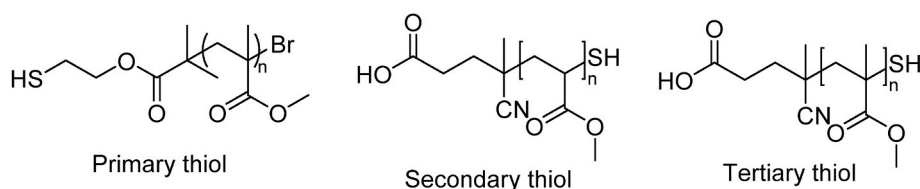
Scheme 3. Structures of each type of side chain polymer.

Scheme 4. Strategies for grafting onto PVDF-based polymers via thiol-ene reactions.

Table 2
List of reactions performed and calculated grafting efficiency. The weight and mole fraction of grafted materials were calculated by NMR integrations.

Sample ID	PVDF backbone	P(M)MA thiol chain-end substitution[a]	Mechanism	Molar fraction of (M)MA	Mass fraction of grafted P(M)MA	P(M)MA chains per PVDF chain
S1	DHF	Primary	Base	0.17	0.25	3.24
S2	DHC			0.17	0.25	3.13
S3	DHF	Secondary[b]		0.18	0.23	4.57
S4	DHC			0.21	0.27	3.91
S5	DHF	Tertiary		0.12	0.18	3.40
S6	DHC			0.03	0.05	0.43
S7	DHF	Primary	Radical	0.11	0.17	2.01
S8	DHC			0.03	0.05	0.54
S9	DHF	Secondary[b]		0.02	0.02	0.36
S10	DHC			0.01	0.01	0.14
S11	DHF	Tertiary		0.03	0.04	0.60
S12	DHC			0.02	0.03	0.26

[a] The molar masses of the P(M)MA side chains ranged from 8000 to 11,000 g/mol; the details are given in Table 1.
[b] The secondary thiols represent PMA–SH instead of PMMA–SH. DHF and DHC refer to the dehydrofluorinated PVDF and dehydrochlorinated PVDF-CTFE, respectively. NMR calculation equations are listed in the Supplementary Information.

thermal stability, as a complementary technique to NMR to further determine the mass of the grafted P(M)MA chains onto DHF-PVDF and DHC-PVDF-CTFE backbones. The onset of thermal degradation is typically defined as the temperature at which 5% weight loss occurs [54]. In this sense, the starting materials represented by the DHF-PVDF and DHC-PVDF-CTFE exhibited the thermal stability of 397 and 388 °C, respectively. They also showed single-stage degradation processes and were used as reference materials for the TGA evaluation. The P(M) MA-grafted analogs generally demonstrated lower thermal stability (depending on the grafted mass and mechanism) due to the presence of less stable grafts. In particular, the samples with high fractions of grafted P(M)MA, mainly achieved by the base-catalyzed reactions (Table 1; S1–S6), exhibited TGA curves with two/more distinct degradation stages. The degradation was therefore evaluated using the differential thermogravimetry (DTG) technique (Fig. 2A). As demonstrated on a representative sample (S1), the first weight loss (284–402 °C) was related to the decomposition of PMMA grafts (determined at T$_{MAX}$), while the second weight loss (385–474 °C) was attributed to the degradation of PVDF backbone. The amounts of grafted PMMA

determined by DTG were in good agreement with those determined by NMR (Fig. 2B). The amounts of grafted PMA, however, could not be precisely determined by DTG due to difficulty separating the degradation of PMA and PVDF, which have overlapping degradation temperatures of 300–450 °C [55] and 422 °C [56] and higher, respectively (DTG analysis shown in Fig. S15). The DTG quantification of PVDF grafted products synthesized by the radical-catalyzed reactions was rather inconclusive due to low amounts of grafted P(M)MA chains (Table 1; S7–S12).

3.4. Crystallinity of grafted PVDF copolymers

A deeper insight into the thermal behavior of prepared DHF-PVDF and DHC-PVDF-CTFE materials and their P(M)MA-grafted analogs was gained using differential scanning calorimetry (DSC). Previous papers dealing exclusively with the PVDF/PMMA blends [51,52,57], reported good miscibility of these polymers, which was attributed to the favorable interaction of hydrogens on PVDF with the carbonyl group of PMMA [58]. Gregorio et al. showed that co-blending of PMMA at
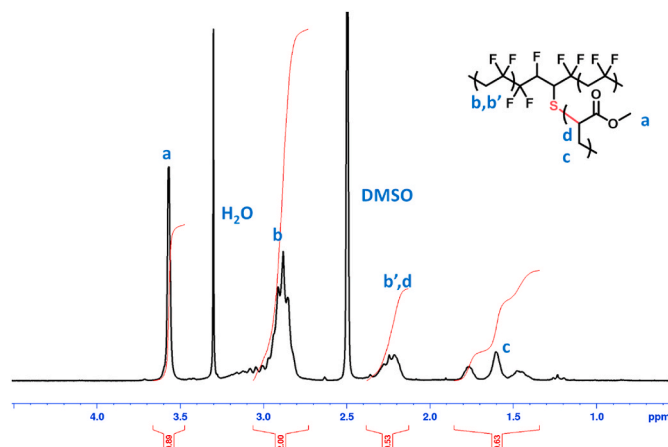
Fig. 1. ¹H NMR of PMA grafted onto DHC-PVDF-CTFE using a base-catalyzed mechanism. Peaks b and b' represent head-tail and head-head/tail-tail arrangements of VDF units, respectively.
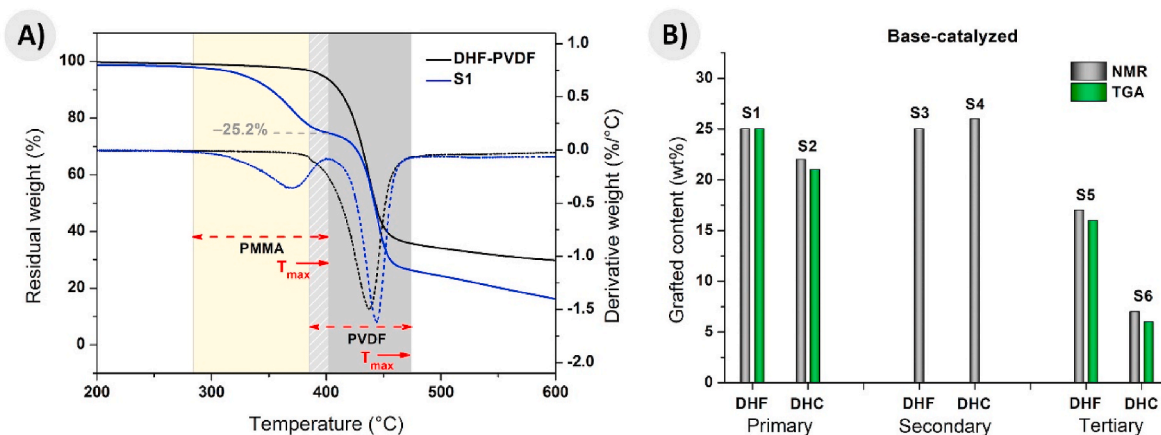
Fig. 2. (A) TGA curves (solid lines) for the DHF-PVDF and its representative PMMA-grafted analogue (S1) and the corresponding DTG analysis (dashed lines) with denoted degradation regions, and their overlapping interval. (B) The comparison of the grafted P(M)MA mass determined by NMR and TGA techniques for the base-catalyzed *grafting-onto* reactions.

Table 3
Overview of the DSC results for the unmodified DHF-PVDF and DHC-PVDF-CTFE, and their P(M)MA grafted products.

Sample ID	PVDF backbone	Thiol substitution	Mechanism	ΔH_C (J/g)	T_C (°C)	ΔH_m (J/g)	T_m (°C)	χ_C (%)
REF-1	DHF	N/D	N/D	23.7	129.4	34.0	160.5	33
REF-2	DHC			10.7	127.6	16.2	160.2, 167.6	16
S1	DHF	Primary	Base	12.0	113.2	16.0	160.1	15
S2	DHC			9.3	124.4	16.3	156.6, 163.7	16
S3	DHF	Secondary[a]		18.1	130.1	22.8	159.1	22
S4	DHC			17.0	124.5	20.4	155.7, 163.2	20
S5	DHF	Tertiary		27.8	119.9	19.9	159.2	19
S6	DHC			11.1	131.2	16.5	162.1, 168.4	16
S7	DHF	Primary	Radical	8.6	121.1	11.4	156.1	11
S8	DHC			10.4	132.5	14.1	163.8, 168.2	13
S9	DHF	Secondary[a]		14.9	129.4	24.8	161.9	24
S10	DHC			11.0	129.8	16.7	160.8, 167.6	16
S11	DHF	Tertiary		13.1	130.0	16.1	160.1	15
S12	DHC			13.8	131.2	9.9	162.2, 168.2	9

[a] The secondary thiols represent PMA–SH instead of PMMA–SH. DHF and DHC refer to the dehydrofluorinated PVDF and dehydrochlorinated PVDF-CTFE, respectively.

concentrations below 15 wt% favored crystallization of the β phase, but the blends became amorphous at PMMA loading above 50 wt%, which presumably impairs the piezoelectric performance [59]. Considering these findings and calculated P(M)MA weight fractions (Table 2), the preserved crystallinity of our PVDF-grafted products was expected despite using, instead of blending, a *grafting onto* fabrication strategy. The degree of crystallinity (χ_C) was calculated following the formula:

$$\chi_c = \frac{\Delta H_m}{\Delta H_m^0} \times 100\% \tag{1}$$

where ΔH_m is the enthalpy of melting, and ΔH_m^0 is the melting enthalpy of 100% crystalline PVDF (104.5 J/g) [60]. DSC results are summarized in Table 2. As seen, the χ_C of the DHF-PVDF was around 33%, which is a similar value compared to that of the conventional PVDF, while the χ_C of the DHC-CTFE-PVDF was significantly lower, at 16% [61]. The χ_C of the DHF-PVDF slightly decreased after grafting with P(M)MA via base-catalyzed reactions (Table 3; S1 and S3), but a more dramatic decrease in χ_C was observed when using the radical-catalyzed mechanism (Table 3; S7, S9 and S11). This finding was rather unexpected, since the radical-catalyzed reactions provided a lower grafting efficiency and, thus, a lower impact on the crystallinity had been anticipated.

The observation can be explained by the role of unsaturated bonds in increasing the crystallinity of polymers. For the base-catalyzed grafted materials, we observe a color change to a darker red/brown of the reaction solution and resulting polymer material. This is indicative of the formation of conjugated segments from additional dehydrofluorination or dehydrochlorination [62]. It has been reported that the unsaturation of polymers can lead to increased crystallization due to the increased rotational stiffness of double bonds [62–64]. As such, the exposure of the

PVDF backbone to TEA can increase the crystallinity of the grafted polymer, relative to radical-catalyzed products due to the generation of new double bonds during the reaction.

For the DHC-CTFE-PVDF backbone, the grafting with P(M)MA via a base-catalyzed mechanism yielded polymers with similar χ_C (16–20%) compared to their parent PVDF analogue (16%), regardless of the type of thiol substitution (Table 3; S2, S4 and S6). The grafting via radical-catalyzed reactions had minimal effect on the χ_C values as well in the case of DHC-CTFE-PVDF (Table 3; S8, S10 and S12). This could be due to the higher reactivity ratio for CTFE than for VDF, as discussed earlier [44,45]. This difference may create polymer chains with lower CTFE content at higher conversion. These species would be less susceptible to the generation of unsaturated sites on the backbone; hence, less grafting would be possible. As such, these species can more easily crystalize, resulting in minimal change in material crystallinity. Overall, it can be concluded that a small fraction of P(M)MA grafts did not distort the alignment of the PVDF during crystallization, yet the *grafting-onto* via base-catalyzed mechanism generally yielded a greater crystallinity of the products.

3.5. Kinetic studies of grafting onto PVDF

Next, we attempted to follow the progress of the base-catalyzed grafting by GPC. The reactions were carried out under the same conditions as sample S4, but in the presence of a polystyrene standard (molar mass, $M_n = 1,052,000$ g/mol, $Đ = 1.06$). For more consistent results, the reaction was diluted twice to ensure good homogeneity in the medium. The aliquots were taken for GPC analysis at different reaction times. The overlapping peaks of PMA-SH and DHC-PVDF-CTFE in the obtained GPC
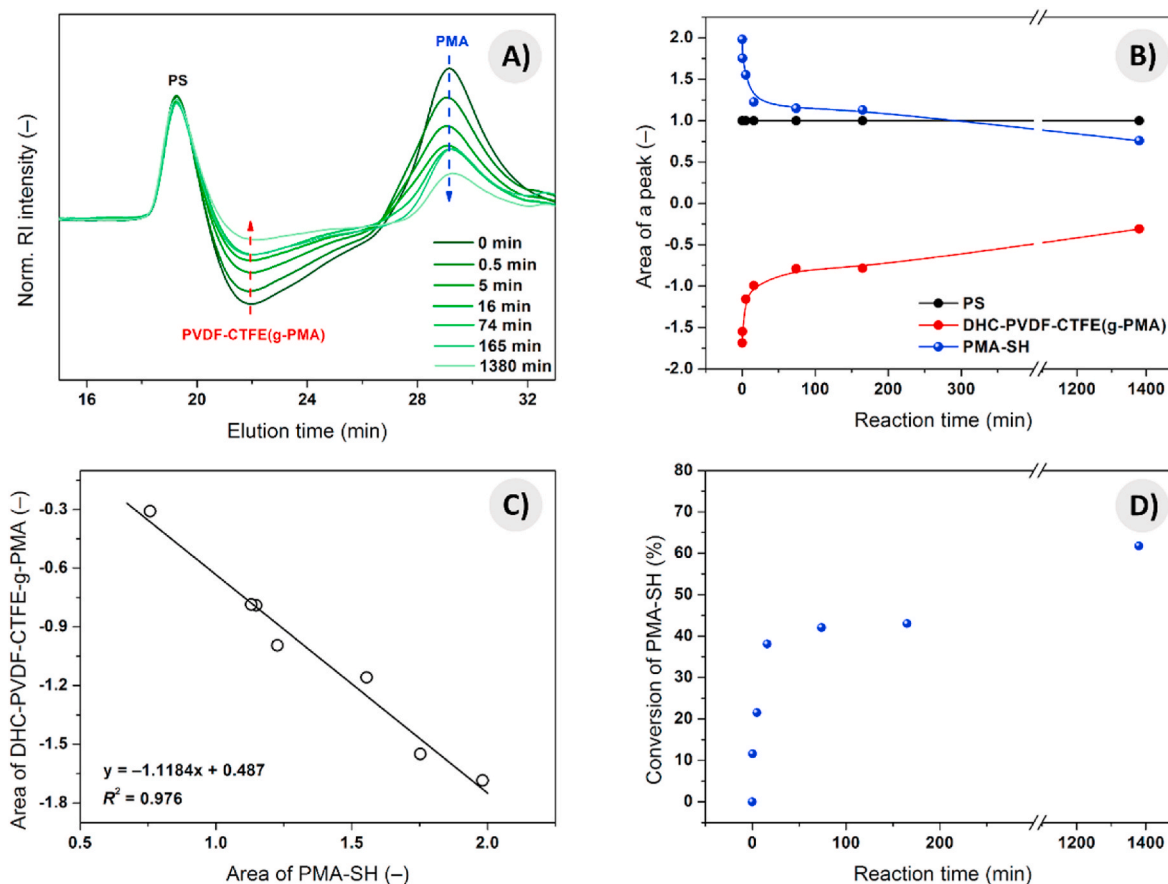
Fig. 3. (A) GPC traces of aliquots from reaction between DHC-PVDF-CTFE and secondary PMA-SH in the presence of TEA normalized against the area of a PS peak as an internal standard (1052 kDa, $Đ = 1.06$). Time zero represents the time of TEA addition; (B) GPC peak areas as a function of reaction time; (C) the area of DHC-PVDF-CTFE(g-PMA) plotted vs. the area of PMA-SH; (D) a calculated conversion plot of PMA-SH over reaction time.

traces were deconvoluted and normalized against the area of PS (Fig. 3A). The signal for PVDF materials appears negative because the refractive index (1.426 for pristine PVDF) is lower than that of DMF (1.430). Over the course of the reaction, the area of the PMA-SH peak gradually decreased, which was attributed to its effective grafting onto the DHC-PVDF-CTFE backbone. This assumption was corroborated by the fact that the peak of DHC-PVDF-CTFE became less negative, which is a consequence of the increasing RI of the grafted product (Fig. 3B). A correlation analysis was performed to confirm that the decrease of the PMA-SH peak resulted in the concurrent incorporation onto DHC-PVDF-CTFE. Fig. 3C shows that using the polystyrene peak as a standard, the decrease of areas of both peaks correlated within 12 % value (slope 1.1184). Thus, this analysis indicates that the PMA-SH polymers were incorporated into fluorinated (co)polymers as grafted side chains. The evolution of the PMA-SH conversion, calculated according to the integrals of PMA-SH peaks, was plotted as a function of reaction time (Fig. 3D). As seen, the thiol-ene reaction was rapid (nearly 40% conversion upon addition of TEA), even though the reactive sites on DHC-PVDF-CTFE are deactivated by fluorine withdrawing groups. The final conversion reached about 70% (obtained after 23h).

Simple Gaussian distributions were selected for the fittings as common practice for deconvoluting polymer GPC peaks in the literature [65, 66]. Using this method, we attempted to estimate the effectiveness of this grafting procedure. Asymmetry and overlap in the peaks indicate that this analysis is not fully quantitative but rather shows qualitative incorporation of PMA to PVDF. Indeed, the changes in the areas of 2 relevant peaks are within 12%: PMA-SH (blue) vs. PVDF (red) (Fig. 3B) and display a slope of 1.12 with a good correlation coefficient, $R^2 = 0.976$. While more complicated distribution models, such as exponential-Gaussian hybrid function (EGH) [67], exponentially modified Gaussian (EMG) [68], or multiple components [69], should be more appropriate for such asymmetric systems, they would necessitate extra parameters in the fitting. This extra complexity would affect the reliability of comparisons between different samples.

An analogous experiment with half the amount of thiol is displayed in Fig. 4. Surprisingly, this experiment also did not lead to quantitative conversion of the thiol, and it stopped at around 70% (normalization by height) or 74% (normalization by area), which is similar to those previously observed with higher amounts of thiol. Therefore, there could be another factor that limited this reaction and should be further investigated.

We hypothesized that the thiol chain ends could have undergone oxidation to form disulfides during storage, resulting in less reactive components. To test this, in-situ reduction of disulfides was performed using tris(hydroxypropyl)phosphine. A small improvement in the conversion of thiolated polymers was observed. However, quantitative conversion was still not achieved. This can be explained by insufficient aminolysis/disulfide reduction of the chain ends due to the bulk of the polymer [70]. Additionally, the oxidation of thiols to disulfides in the presence of oxygen is catalyzed under basic conditions, which necessarily yields a fraction of disulfides present in the reaction mixture, lowering grafting efficiency [71–73].

In summary, we have systematically screened the effect of thiol-ene reaction conditions (radical and basic) and substitution of each thiol chain-end terminated poly(meth)acrylates (primary, secondary, and tertiary) on the grafting efficiency. The results indicated an order of magnitude higher yields under basic conditions. The primary and secondary thiols were most reactive. This chemistry could be expanded to other grafted side chains for different applications; they should be soluble in the same solvents as PVDF. One limitation of this method is the synthesis of densely grafted copolymers. Additionally, it will be interesting to explore the grafting-onto process with surfaces of PVDF under heterogeneous conditions. Surface grafting would better preserve the crystallinity of the sample and, in turn, its piezoelectricity, as well as broaden the scope of side chains.

4. Conclusions

Herein, different reaction conditions for grafting poly(meth)acrylates onto PVDF were explored, including the effects of different PVDF backbones, the steric effects of the side chains, and base-versus radical-catalyzed thiol-ene reaction mechanisms. The grafting efficiency of the products was determined by a combination of NMR, TGA, and GPC. Grafting density was an order of magnitude higher under basic conditions compared to the analogous UV-catalyzed radical reactions. Additionally, primary and secondary thiols showed the highest grafting efficiency, which was attributed to their favorably diminished steric effects. A slightly higher grafting density was observed in DHF-PVDF than in DHC-PVDF-CTFE. It was found that up to 4 side chains of P(M)MA could be grafted onto one PVDF chain. Sparse grafting of the side chains still allowed the PVDF backbone to crystallize, as determined by DSC.

5. Future directions

Using the presented chemical strategy, other side chains with various functionalities could plausibly be grafted onto PVDF-based materials, expanding and optimizing the application scope of these materials while preserving favorable PVDF properties such as robustness and crystallinity. PVDF is commonly used in water filtration membranes but is susceptible to biofouling due to its inherent hydrophobicity. Modification of PVDF membranes with hydrophilic side chains such as poly(oligo
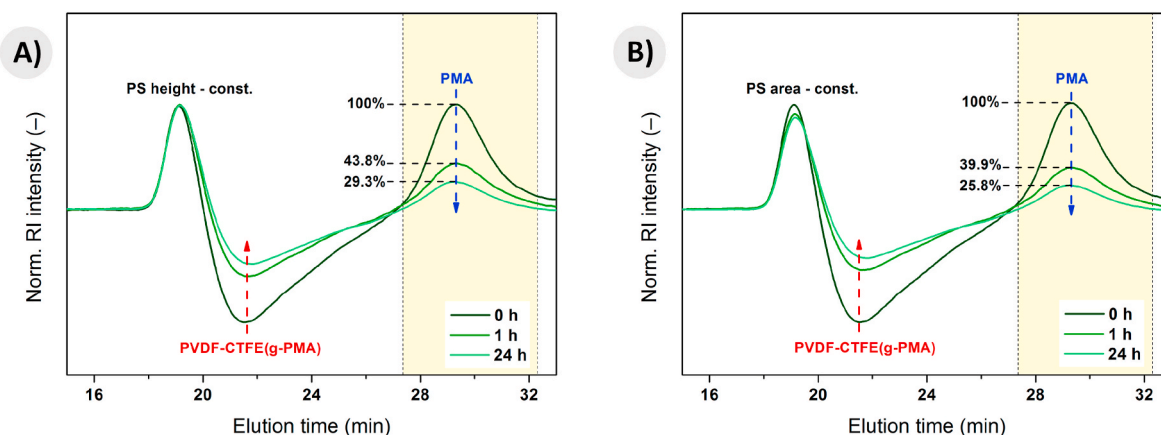

Fig. 4. GPC traces of the grafting experiment using half the amount of PMA-SH (secondary thiol). The progress of the reaction was determined as a decrease in the PMA area after the normalization of curves by (A) PS peak height and (B) its area. The denoted region represents the limits of PMA integration.

(ethylene oxide) methyl ether methacrylate) or poly(*N*-iso-propylacrylamide) could enhance their performance without detriment to the membrane's stability. PVDF is also used as a lithium-ion battery binder, due to its aforementioned chemical and thermal stability. PVDF binders can be modified with poly(acrylic acid) and a charge carrier such as poly(2-acrylamido-2-methyl-1-propanesulfonic acid) to enhance performance.

Despite its shortcomings, grafting from PVDF using ATRP is still a viable option for making PVDF graft copolymers. Different ATRP techniques, such as surface-initiated ATRP and oxygen-tolerant ATRP, are facile methods to modify a chemically robust material. Grafting from, and now onto, PVDF are techniques that allow tailoring of materials through control of grafting density and graft lengths, thus broadening the application scope of PVDF.

CRediT authorship contribution statement

Ting-Chih Lin: Writing – review & editing, Writing – original draft, Visualization, Investigation, Conceptualization. **Piotr Mocny:** Writing – review & editing, Visualization, Investigation. **Martin Cvek:** Writing – review & editing, Visualization, Investigation. **Mingkang Sun:** Investigation, Conceptualization. **Krzysztof Matyjaszewski:** Writing – review & editing, Writing – original draft, Supervision, Conceptualization.

Declaration of competing interest

The authors declare the following financial interests/personal relationships which may be considered as potential competing interests: K Matyjaszewski reports financial support was provided by National Science Foundation.

Data availability

Data will be made available on request.

Acknowledgments

Appendix A. Supplementary data

Supplementary data to this article can be found online at https://doi.org/10.1016/j.polymer.2024.126848.

References

[1] G. Zapsas, Y. Patil, Y. Gnanou, B. Ameduri, N. Hadjichristidis, Poly(vinylidene fluoride)-based complex macromolecular architectures: from synthesis to properties and applications, Prog. Polym. Sci. 104 (2020) 101231, https://doi.org/10.1016/j.progpolymsci.2020.101231.

[2] B. Ameduri, From vinylidene fluoride (VDF) to the applications of VDF-containing polymers and copolymers: recent developments and future trends, Chem. Rev. 109 (12) (2009) 6632–6686, https://doi.org/10.1021/cr800187m.

[3] E. Leivo, T. Wilenius, T. Kinos, P. Vuoristo, T. Mäntylä, Properties of thermally sprayed fluoropolymer PVDF, ECTFE, PFA and FEP coatings, Prog. Org. Coating 49 (1) (2004) 69–73, https://doi.org/10.1016/j.porgcoat.2003.08.011.

[4] J.K. Koh, Y.W. Kim, S.H. Ahn, B.R. Min, J.H. Kim, Antifouling poly(vinylidene fluoride) ultrafiltration membranes containing amphiphilic comb polymer additive, J. Polym. Sci., Part B: Polym. Phys. 48 (2) (2010) 183–189, https://doi.org/10.1002/polb.21887.

[5] Y. Tong, L. Huang, C. Zuo, W. Li, W. Xing, Novel PVDF-g-NMA copolymer for fabricating the hydrophilic ultrafiltration membrane with good antifouling property, Ind. Eng. Chem. Res. 60 (1) (2021) 541–550, https://doi.org/10.1021/acs.iecr.0c04303.

[6] Q. Wu, A. Tiraferri, T. Li, W. Xie, H. Chang, Y. Bai, B. Liu, Superwettable PVDF/PVDF-g-PEGMA ultrafiltration membranes, ACS Omega 5 (36) (2020) 23450–23459, https://doi.org/10.1021/acsomega.0c03429.

[7] B. Ameduri, Copolymers of vinylidene fluoride with functional comonomers and applications therefrom: recent developments, challenges and future trends, Prog. Polym. Sci. 133 (2022) 101591, https://doi.org/10.1016/j.progpolymsci.2022.101591.

[8] G.-d. Kang, Y.-m. Cao, Application and modification of poly(vinylidene fluoride) (PVDF) membranes – a review, J. Membr. Sci. 463 (2014) 145–165, https://doi.org/10.1016/j.memsci.2014.03.055.

[9] J.-I. Lee, H. Kang, K.H. Park, M. Shin, D. Hong, H.J. Cho, N.-R. Kang, J. Lee, S. M. Lee, J.-Y. Kim, C.K. Kim, H. Park, N.-S. Choi, S. Park, C. Yang, Amphiphilic graft copolymers as a versatile binder for various electrodes of high-performance lithium-ion batteries, Small 12 (23) (2016) 3119–3127, https://doi.org/10.1002/smll.201600800.

[10] H.-H. Gong, Y. Zhang, Y.-P. Cheng, M.-X. Lei, Z.-C. Zhang, The application of controlled/living radical polymerization in modification of PVDF-based fluoropolymer, Chin. J. Polym. Sci. 39 (9) (2021) 1110–1126, https://doi.org/10.1007/s10118-021-2616-x.

[11] J.F. Hester, P. Banerjee, Y.Y. Won, A. Akthakul, M.H. Acar, A.M. Mayes, ATRP of amphiphilic graft copolymers based on PVDF and their use as membrane additives, Macromolecules 35 (20) (2002) 7652–7661, https://doi.org/10.1021/ma0122270.

[12] S. Holmberg, P. Holmlund, R. Nicolas, C.-E. Wilén, T. Kallio, G. Sundholm, F. Sundholm, Versatile synthetic route to tailor-made proton exchange membranes for fuel cell applications by combination of radiation chemistry of polymers with nitroxide-mediated living free radical graft polymerization, Macromolecules 37 (26) (2004) 9909–9915, https://doi.org/10.1021/ma0353641.

[13] H. Zhao, S. Ren, I. Zucker, Y. Bai, Y. Wang, Antibiofouling polyvinylidene fluoride membrane functionalized by poly(ionic liquid) brushes via atom transfer radical polymerization, ACS ES&T EngACS ES&T Engg.g (2022), https://doi.org/10.1021/acsestengg.1c00440.

[14] K.A. Davis, K. Matyjaszewski, Statistical, Gradient and Segmented Copolymers by Controlled/Living Radical Polymerizations, Springer Verlag, Berlin, 2002.

[15] G. Xie, M.R. Martinez, M. Olszewski, S.S. Sheiko, K. Matyjaszewski, Molecular bottlebrushes as novel materials, Biomacromolecules 20 (1) (2019) 27–54, https://doi.org/10.1021/acs.biomac.8b01171.

[16] L. Sauguet, C. Boyer, B. Ameduri, B. Boutevin, Synthesis and characterization of poly(vinylidene fluoride)-g-poly(styrene) graft polymers obtained by atom transfer radical polymerization of styrene, Macromolecules 39 (26) (2006) 9087–9101, https://doi.org/10.1021/ma061554a.

[17] M. Guerre, M. Semsarilar, V. Ladmiral, Grafting from fluoropolymers using ATRP: what is missing? Eur. J. Inorg. Chem. 2022 (4) (2022) e202100945 https://doi.org/10.1002/ejic.202100945.

[18] S. Lanzalaco, M. Fantin, O. Scialdone, A. Galia, A.A. Isse, A. Gennaro, K. Matyjaszewski, Atom transfer radical polymerization with different halides (F, Cl, Br, and I): is the process "living" in the presence of fluorinated initiators? Macromolecules 50 (1) (2017) 192–202, https://doi.org/10.1021/acs.macromol.6b02286.

[19] H. Kise, H. Ogata, Phase transfer catalysis in dehydrofluorination of poly (vinylidene fluoride) by aqueous sodium hydroxide solutions, J. Polym. Sci. Polym. Chem. Ed. 21 (12) (1983) 3443–3451, https://doi.org/10.1002/pol.1983.170211208.

[20] A.J. Dias, T.J. McCarthy, Dehydrofluorination of poly(vinylidene fluoride) in dimethylformamide solution: synthesis of an operationally soluble semiconducting polymer, J. Polym. Sci. Polym. Chem. Ed. 23 (4) (1985) 1057–1061, https://doi.org/10.1002/pol.1985.170230410.

[21] H. Kise, M. Sugihara, F.-F. He, Electrical conductivity of chemically dehydrochlorinated poly(vinyl chloride) films doped with electron acceptors, J. Appl. Polym. Sci. 30 (3) (1985) 1133–1143, https://doi.org/10.1002/app.1985.070300319.

[22] K.W. Kang, C.W. Hwang, T.S. Hwang, Synthesis and properties of sodium vinylbenzene sulfonate-grafted poly(vinylidene fluoride) cation exchange membranes for membrane capacitive deionization process, Macromol. Res. 23 (12) (2015) 1126–1133, https://doi.org/10.1007/s13233-015-3153-7.

[23] Y. Zhu, J. Wang, F. Zhang, S. Gao, A. Wang, W. Fang, J. Jin, Zwitterionic nanohydrogel grafted PVDF membranes with comprehensive antifouling property and superior cycle stability for oil-in-water emulsion separation, Adv. Funct. Mater. 28 (40) (2018) 1804121, https://doi.org/10.1002/adfm.201804121.

[24] L. Xiao, D.M. Davenport, L. Ormsbee, D. Bhattacharyya, Polymerization and functionalization of membrane pores for water related applications, Ind. Eng. Chem. Res. 54 (16) (2015) 4174–4182, https://doi.org/10.1021/ie504149t.

[25] R. Wang, Y. Duan, X. Xiong, Preparation of hydrophilic poly(vinylidene fluoride) membrane by in-situ grafting of N-vinyl pyrrolidone via a reactive vapor induced phase separation procedure, J. Polym. Sci., Part A: Polym. Chem. 59 (20) (2021) 2284–2294, https://doi.org/10.1002/pol.20210446.

[26] K.S. Jeong, W.C. Hwang, T.S. Hwang, Synthesis of an aminated poly(vinylidene fluride-g-4-vinyl benzyl chloride) anion exchange membrane for membrane capacitive deionization(MCDI), J. Membr. Sci. 495 (2015) 316–321, https://doi.org/10.1016/j.memsci.2015.08.005.

[27] J. Liu, X. Shen, Y. Zhao, L. Chen, Acryloylmorpholine-grafted PVDF membrane with improved protein fouling resistance, Ind. Eng. Chem. Res. 52 (51) (2013) 18392–18400, https://doi.org/10.1021/ie403456n.

[28] H. Sun, X. Zhang, Y. He, D. Zhang, X. Feng, Y. Zhao, L. Chen, Preparation of PVDF-g-PAA-PAMAM membrane for efficient removal of copper ions, Chem. Eng. Sci. 209 (2019) 115186, https://doi.org/10.1016/j.ces.2019.115186.

[29] S. Tan, J. Li, G. Gao, H. Li, Z. Zhang, Synthesis of fluoropolymer containing tunable unsaturation by a controlled dehydrochlorination of P(VDF-co-CTFE) and its curing for high performance rubber applications, J. Mater. Chem. 22 (35) (2012) 18496–18504, https://doi.org/10.1039/C2JM33133K.

[30] M. Sharma, N. Padmavathy, S. Remanan, G. Madras, S. Bose, Facile one-pot scalable strategy to engineer biocidal silver nanocluster assembly on thiolated PVDF membranes for water purification, RSC Adv. 6 (45) (2016) 38972–38983, https://doi.org/10.1039/C6RA03143A.

[31] S. Owusu-Nkwantabisah, M. Robbins, D.Y. Wang, Towards superhydrophobic coatings via thiol-ene post-modification of polymeric submicron particles, Appl. Surf. Sci. 450 (2018) 164–169, https://doi.org/10.1016/j.apsusc.2018.04.182.

[32] S. Tan, D. Li, Y. Zhang, Z. Niu, Z. Zhang, Base catalyzed thiol–ene click chemistry toward inner CH_2CF_2 bonds for controlled functionalization of poly(vinylidene fluoride), Macromol. Chem. Phys. 219 (11) (2018) 1700632, https://doi.org/10.1002/macp.201700632.

[33] M. Wang, J. Liao, B. Peng, Y. Zhang, S. Tan, Z. Zhang, Facile grafting modification of poly(vinylidene fluoride-co-trifluoroethylene) directly from inner CH_2CH bonds, Macromol. Chem. Phys. 222 (8) (2021) 2100017, https://doi.org/10.1002/macp.202100017.

[34] J. Hu, S. Yuan, W. Zhao, C. Li, P. Liu, X. Shen, Fabrication of a superhydrophilic/superoleophobic PVDF membrane via thiol–ene photochemistry for the oil/water separation, Colloids Surf., A 664 (2023) 131138, https://doi.org/10.1016/j.colsurfa.2023.131138.

[35] H. He, S. Averick, E. Roth, D. Luebke, H. Nulwala, K. Matyjaszewski, Clickable poly (ionic liquid)s for modification of glass and silicon surfaces, Polymer 55 (2014) 3330–3338, https://doi.org/10.1016/j.polymer.2014.01.045.

[36] C.E. Hoyle, C.N. Bowman, Thiol–ene click chemistry, Angew. Chem., Int. Ed. 49 (9) (2010) 1540–1573, https://doi.org/10.1002/anie.200903924.

[37] B.D. Mather, K. Viswanathan, K.M. Miller, T.E. Long, Michael addition reactions in macromolecular design for emerging technologies, Prog. Polym. Sci. 31 (5) (2006) 487–531, https://doi.org/10.1016/j.progpolymsci.2006.03.001.

[38] E. Mueller, I. Poulin, W.J. Bodnaryk, T. Hoare, Click chemistry hydrogels for extrusion bioprinting: progress, challenges, and opportunities, Biomacromolecules 23 (3) (2022) 619–640, https://doi.org/10.1021/acs.biomac.1c01105.

[39] A. Taguet, B. Ameduri, B. Boutevin, Crosslinking of Vinylidene Fluoride-Containing Fluoropolymers, Crosslinking in Materials Science, Springer, Berlin, Heidelberg, 2005, pp. 127–211.

[40] A. Staccione, M. Albano, Curable Fluoroelastomers, Solvay Solexis SpA, 2003.

[41] H. Kise, H. Ogata, M. Nakata, Chemical dehydrofluorination and electrical conductivity of poly(vinylidene fluoride) films, Angew. Makromol. Chem. 168 (1) (1989) 205–216, https://doi.org/10.1002/apmc.1989.051680117.

[42] S. Samanta, D.P. Chatterjee, S. Manna, A. Mandal, A. Garai, A.K. Nandi, Multifunctional hydrophilic poly(vinylidene fluoride) graft copolymer with supertoughness and supergluing properties, Macromolecules 42 (8) (2009) 3112–3120, https://doi.org/10.1021/ma9003117.

[43] G. Moggi, P. Bonardelli, J.C.J. Bart, Copolymers of 1,1-difluoroethene with tetrafluoroethene, chlorotrifluoroethene, and bromotrifluoroethene, J. Polym. Sci., Polym. Phys. Ed. 22 (3) (1984) 357–365, https://doi.org/10.1002/pol.1984.180220303.

[44] J.E. Dohany, J.S. Humphrey, Encyclopedia of Polymer Science and Engineering, Encyclopedia of Polymer Science and Engineering, Wiley, New York, 1989, pp. 532–548.

[45] T. Soulestin, Synthesis and Characterizations of New Fluorinated Electroactive Copolymers, University of Montpellier, 2016. PhD Dissertation.

[46] A.B. Lowe, Thiol-ene "click" reactions and recent applications in polymer and materials synthesis, Polym. Chem. 1 (1) (2010) 17–36, https://doi.org/10.1039/B9PY00216B.

[47] L.A. Navarro, A.E. Enciso, K. Matyjaszewski, S. Zauscher, Enzymatically degassed surface-initiated atom transfer radical polymerization with real-time monitoring, J. Am. Chem. Soc. 141 (7) (2019) 3100–3109, https://doi.org/10.1021/jacs.8b12072.

[48] M. Kobayashi, Y. Higaki, T. Kimura, F. Boschet, A. Takahara, B. Ameduri, Direct surface modification of poly(VDF-co-TrFE) films by surface-initiated ATRP without pretreatment, RSC Adv. 6 (89) (2016) 86373–86384, https://doi.org/10.1039/C6RA18397B.

[49] Y. Chen, W. Sun, Q. Deng, L. Chen, Controlled grafting from poly(vinylidene fluoride) films by surface-initiated reversible addition–fragmentation chain transfer polymerization, J. Polym. Sci., Part A: Polym. Chem. 44 (9) (2006) 3071–3082, https://doi.org/10.1002/pola.21410.

[50] H. Gao, K. Matyjaszewski, Synthesis of molecular brushes by "Grafting onto" method: combination of ATRP and click reactions, J. Am. Chem. Soc. 129 (20) (2007) 6633–6639, https://doi.org/10.1021/ja0711617.

[51] W.-K. Lee, C.-S. Ha, Miscibility and surface crystal morphology of blends containing poly(vinylidene fluoride) by atomic force microscopy, Polymer 39 (26) (1998) 7131–7134, https://doi.org/10.1016/S0032-3861(97)10081-7.

[52] H. Sasaki, P. Kanti Bala, H. Yoshida, E. Ito, Miscibility of PVDF/PMMA blends examined by crystallization dynamics, Polymer 36 (25) (1995) 4805–4810, https://doi.org/10.1016/0032-3861(95)99296-7.

[53] M.D. Nothling, Q. Fu, A. Reyhani, S. Allison-Logan, K. Jung, J. Zhu, M. Kamigaito, C. Boyer, G.G. Qiao, Progress and perspectives beyond traditional RAFT polymerization, Adv. Sci. 7 (20) (2020) 2001656, https://doi.org/10.1002/advs.202001656.

[54] W. Li, H. Li, Y.-M. Zhang, Preparation and investigation of PVDF/PMMA/TiO2 composite film, J. Mater. Sci. 44 (11) (2009) 2977–2984, https://doi.org/10.1007/s10853-009-3395-x.

[55] A. Kubotera, R. Saito, Synthesis of well-defined 3-arm and 6-arm poly(acrylic acid) s via ATRP of methyl acrylate and hydrolyses of 3-arm and 6-arm poly(methyl acrylate)s, Polym. J. 48 (5) (2016) 611–619, https://doi.org/10.1038/pj.2015.133.

[56] M.C. Rehwoldt, Y. Wang, F. Xu, P. Ghildiyal, M.R. Zachariah, High-temperature interactions of metal oxides and a PVDF binder, ACS Appl. Mater. Interfaces 14 (7) (2022) 8938–8946, https://doi.org/10.1021/acsami.1c20938.

[57] H. Song, S. Yang, S. Sun, H. Zhang, Effect of miscibility and crystallization on the mechanical properties and transparency of PVDF/PMMA blends, Polym.-Plast. Technol. Eng. 52 (3) (2013) 221–227, https://doi.org/10.1080/03602559.2012.735314.

[58] C. Léonard, J.L. Halary, L. Monnerie, Hydrogen bonding in PMMA-fluorinated polymer blends: FTi.r. investigations using ester model molecules, Polymer 26 (10) (1985) 1507–1513, https://doi.org/10.1016/0032-3861(85)90084-9.

[59] J.R. Gregorio, N.C.P.d.S. Nociti, Effect of PMMA addition on the solution crystallization of the alpha and beta phases of poly(vinylidene fluoride) (PVDF), J. Phys. D Appl. Phys. 28 (2) (1995) 432, https://doi.org/10.1088/0022-3727/28/2/028.

[60] K. Nakagawa, Y. Ishida, Annealing effects in poly(vinylidene fluoride) as revealed by specific volume measurements, differential scanning calorimetry, and electron microscopy, J. Polym. Sci., Polym. Phys. Ed. 11 (11) (1973) 2153–2171, https://doi.org/10.1002/pol.1973.180111107.

[61] A. Gebrekrstos, G. Prasanna Kar, G. Madras, A. Misra, S. Bose, Does the nature of chemically grafted polymer onto PVDF decide the extent of electroactive β-polymorph? Polymer 181 (2019) 121764 https://doi.org/10.1016/j.polymer.2019.121764.

[62] J. Lin, M.H. Malakooti, H.A. Sodano, Thermally stable poly(vinylidene fluoride) for high-performance printable piezoelectric devices, ACS Appl. Mater. Interfaces 12 (19) (2020) 21871–21882, https://doi.org/10.1021/acsami.0c03675.

[63] L. Groo, D.J. Inman, H.A. Sodano, Dehydrofluorinated PVDF for structural health monitoring in fiber reinforced composites, Compos. Sci. Technol. 214 (2021) 108982, https://doi.org/10.1016/j.compscitech.2021.108982.

[64] Y. Wang, H. Wang, K. Liu, T. Wang, C. Yuan, H. Yang, Effect of dehydrofluorination reaction on structure and properties of PVDF electrospun fibers, RSC Adv. 11 (49) (2021) 30734–30743, https://doi.org/10.1039/D1RA05667K.

[65] M. Semsarilar, E.R. Jones, S.P. Armes, Comparison of pseudo-living character of RAFT polymerizations conducted under homogeneous and heterogeneous conditions, Polym. Chem. 5 (1) (2014) 195–203, https://doi.org/10.1039/C3PY01042B.

[66] N. De Alwis Watuthanthrige, J.A. Reeves, M.T. Dolan, S. Valloppilly, M.B. Zanjani, Z. Ye, D. Konkolewicz, Wavelength-controlled synthesis and degradation of thermoplastic elastomers based on intrinsically photoresponsive phenyl vinyl ketone, Macromolecules 53 (13) (2020) 5199–5207, https://doi.org/10.1021/acs.macromol.0c00401.

[67] K. Lan, J.W. Jorgenson, A hybrid of exponential and Gaussian functions as a simple model of asymmetric chromatographic peaks, J. Chromatogr. A 915 (1) (2001) 1–13, https://doi.org/10.1016/S0021-9673(01)00594-5.

[68] E. Grushka, Characterization of exponentially modified Gaussian peaks in chromatography, Anal. Chem. 44 (11) (1972) 1733–1738, https://doi.org/10.1021/ac60319a011.

[69] Y.V. Kissin, Molecular weight distributions of linear polymers: detailed analysis from GPC data, J. Polym. Sci. Polym. Chem. 33 (2) (1995) 227–237, https://doi.org/10.1002/pola.1995.080330205.

[70] G.-Z. Li, R.K. Randev, A.H. Soeriyadi, G. Rees, C. Boyer, Z. Tong, T.P. Davis, C. R. Becer, D.M. Haddleton, Investigation into thiol-(meth)acrylate Michael addition reactions using amine and phosphine catalysts, Polym. Chem. 1 (8) (2010) 1196–1204, https://doi.org/10.1039/C0PY00100G.

[71] M. Oba, K. Tanaka, K. Nishiyama, W. Ando, Aerobic oxidation of thiols to disulfides catalyzed by diaryl tellurides under photosensitized conditions, J. Org. Chem. 76 (10) (2011) 4173–4177, https://doi.org/10.1021/jo200496r.

[72] D. Schilter, Thiol oxidation: a slippery slope, Nat. Rev. Chem 1 (2) (2017) 0013, https://doi.org/10.1038/s41570-016-0013.

[73] X. Qiu, X. Yang, Y. Zhang, S. Song, N. Jiao, Efficient and practical synthesis of unsymmetrical disulfides via base-catalyzed aerobic oxidative dehydrogenative coupling of thiols, Org. Chem. Front. 6 (13) (2019) 2220–2225, https://doi.org/10.1039/C9QO00239A.